Effect of Titanium Dioxide Particles on the Surface Morphology and the Mechanical Properties of PVC Composites During QUV Accelerated Weathering

Teng-Chun Yang,[1,2] Takafumi Noguchi,[2] Minoru Isshiki,[3] Jyh-Horng Wu[1]
[1]*Department of Forestry, National Chung Hsing University, Taichung 402, Taiwan*

[2]*Department of Architecture, School of Engineering, The University of Tokyo, Tokyo 113, Japan*

[3]*Vinyl Environmental Council, Chuo-ku, Tokyo 104, Japan*

In this study, QUV accelerated weathering of polyvinyl chloride (PVC) composites with different amounts of titanium dioxide (TiO_2) particle was conducted to investigate the effect of TiO_2 particle on the surface morphology and the mechanical properties. The results indicate that the surface morphology of PVC without TiO_2 particle did not exhibit changes up to 960 h, but exhibited a rough and brittle surface after 1920 h of QUV accelerated weathering. In addition, the tan δ intensity, the elongation at break, and the mean failure energy (MFE) decreased significantly with increasing exposure time due to embrittlement. In contrast, for TiO_2 particle-loaded PVCs, no significant influence on the tan δ intensity and the mechanical properties after accelerated weathering were observed, despite the appreciable degradation that occurred in the surface layer. The weatherability, as determined by the mechanical performance, was improved with increasing loading of TiO_2 particle in the PVC composites. Although the TiO_2 particle in the PVC matrix acts as a photocatalyst to enhance the surface degradation, it is also an effective radiation screener that inhibits embrittlement and retards the decrease in mechanical properties caused by the accelerated weathering process. POLYM. COMPOS., 37:3391–3397, 2016. © 2015 Society of Plastics Engineers

INTRODUCTION

Polyvinyl chloride (PVC), which was initially developed over a century ago, remains a material that is indispensable to daily life despite the development of a variety of polymer materials in the plastics industry. According to the statistics of the Ministry of Economy, Trade and Industry (METI) of Japan in 2013 [1], the demand for PVC in the entire world achieved approximately 36 million tons, with over half of the PVC used in Asia (19 million tons). The basic features of PVC are the presence of chlorine in the configuration element and a random coil in the molecular state. Accordingly, the nature of PVC makes it superior in terms of durability, moldability, fire retardant capability, and compatibility compared to other commodity plastics. In addition, the quality of design of PVC is highlighted by the ability to produce a hard or soft material with the advantages of printability, boning capability, second workability, on-site construction, and recyclability. Validation of the benefits of these features is highlighted by the ability of PVC to be used in a very wide range of applications [2].

In building construction, PVC has been used worldwide for outdoor applications, such as siding, pipes, and window profiles, because of its low cost, economic efficiency, and high durability. However, the principle pathways of photodegradation for PVC are the generation of the polyene structure due to dehydrochlorination and the production of a variety of carbonyl due to oxidative degradation [3–5]. It is well-known that polymers gradually degrade under environmental stress, as indicated by changes in color, gloss, mechanical properties, etc. [6–8]. Therefore, stabilizers and pigments are added in PVC to protect it from UV irradiation. The most essential additive for PVC material designed to perform outdoors is titanium dioxide (TiO_2) due to its excellent UV absorption and barrier properties [9–11]. For most applications, TiO_2 has been used to improve the opacity, appearance, and durability of PVC products [12–14]. However, Day [15] reported that TiO_2 is also a photoreactive material. TiO_2 can accelerate the degradation of the surface of PVC when it is activated by UV, water, and oxygen. The photoreactive process in TiO_2 is as follows. Absorption of UV irradiation in TiO_2 promotes electrons from the valence band into the conduction band,

Correspondence to: J.-H. Wu; e-mail: eric@nchu.edu.tw
DOI 10.1002/pc.23537
Published online in Wiley Online Library (wileyonlinelibrary.com).

leaving behind holes in the valence band. These electron-hole pairs promote oxidation-reduction reactions with the polymer material and/or undergo interfacial charge transfer with the surface or adsorbed species to form reactive radicals [16, 17].

Over the past few decades, a few researchers [3–5, 18–20] have studied the degradation products and photo-oxidation mechanisms of PVC incorporated additives under various weathering conditions; however, these research studies were primarily confined to a film specimen exposed to xenon-arc radiation with and without water spray. In our previous study [21], we demonstrated that TiO_2 particle in PVC composites inhibits photo-oxidation and chain scission during QUV accelerated weathering. However, there is a lack of detailed information on the macromolecular changes and the mechanical properties of bulk PVC composites with or without TiO_2 particle under the QUV accelerated weathering. Therefore, the present study involves an in-depth investigation on the influence of TiO_2 particle on the surface morphology, dynamic mechanical properties, tensile properties, and impact properties of PVC composites during QUV accelerated weathering.

EXPERIMENTAL

Material and Specimen Preparation

Compression-molded 1-mm thick PVC specimens (Kane Vinyl S1001) were supplied by Kaneka Co. (Japan). The PVC matrix contained additives that were similar to those used in PVC for outdoor applications. The formulation of PVC composites contains 100 phr PVC (Kane Vinyl S1001), 0.7 phr of acrylic polymer (Kane Ace PA-20, Kaneka, Japan), 0.5 phr of paraffin wax (Luvax-1266, Nippon Seiro, Japan), 0.6 phr of organotin mercaptide (TM-181 FS, Dow Chemical, USA), and 1.5 phr of fatty acid soap (calcium stearate and zinc stearate) [22]. In addition, TiO_2 particle (R-105, DuPont, USA) is used as an inorganic pigment. In this study, TiO_2 particle was incorporated into PVC composites as 0 phr, 5 phr, and 10 phr loadings named as PVC(T_0), PVC(T_5), and PVC(T_{10}), respectively.

Accelerated Weathering Test

Accelerated weathering was conducted in a QUV tester using fluorescent lamps UVA-340 (Q-Lab, USA). The varying spectral energy distribution provided the best possible simulation of sunlight over the critical short wavelength region from 365 nm to the solar cutoff of 295 nm. The irradiance of the peak emission was 0.68 W/m^2 at 340 nm. This wavelength is significant in the accelerated degradation of PVC because PVC only absorbs irradiation from 310 to 370 nm. The test cycle in this study consisted of 8 h of UV exposure at 50 ± 3 °C and 4 h in the dark with condensation at the same temperature. A complete test lasted 1920 h (80 days). All weathered specimens were air-dried in ambient conditions for 24 h before measuring the various properties.

Scanning Electron Microscopy (SEM)

After sputter coating the specimens with platinum, the surface morphological images of PVC composites were examined by scanning electron microscopy (SEM, JSM-6701F, JEOL, Japan) at an accelerating voltage of 3.0 kV.

Dynamic Mechanical Analysis (DMA)

The dynamic mechanical properties of the PVC composites were measured via Dynamic Mechanical Analysis (DMA) in single-cantilever bending mode (DMA 8000, Perkin-Elmer, UK) at a heating rate of 5 °C/min and a frequency of 1 Hz. The storage modulus (E') and loss tangent (tan δ) were recorded over a temperature range of $25 - 125$ °C. The dimensions of the specimens were 17 mm $\times$ 10 mm with a thickness of 1.0 mm.

Mechanical Properties

The tensile testing (Autograph AG-X, Shimadzu, Japan) was performed at a rate of 10 mm/min according to the ASTM D638 standard on standard type I dumbbell-shaped specimens. Evaluation of the impact strength was in accordance with ASTM D4226, using a puncture impact strength tester (SPI Modified Impact Tester, BYK, Germany) to calculate the mean failure energy (MFE).

Static Analysis

All of the results were expressed in the form of a mean $\pm$ SD. The significance of difference was calculated using Scheffe's test, and P values < 0.05 were considered to be significant.

RESULTS AND DISCUSSION

Surface Morphology

The generation of an oxidation layer on the surface of plastics during weathering is well-known, but very few literature reports focused on the changes in surface morphology as a function of TiO_2 particle loading amount. Therefore, in this study, images of the surface morphology of PVC composites with 5 phr and 10 phr of TiO_2 were observed by SEM during the accelerated weathering process. Figure 1 shows that, except for some defects caused by the manufacturing process, all specimen surfaces were relatively smooth before accelerated weathering test. For the PVC(T_0), no significant changes were observed up to 960 h (Fig. 1A–C). However, after 1920 h of weathering, the surface became unsmooth and

 DOI 10.1002/pc

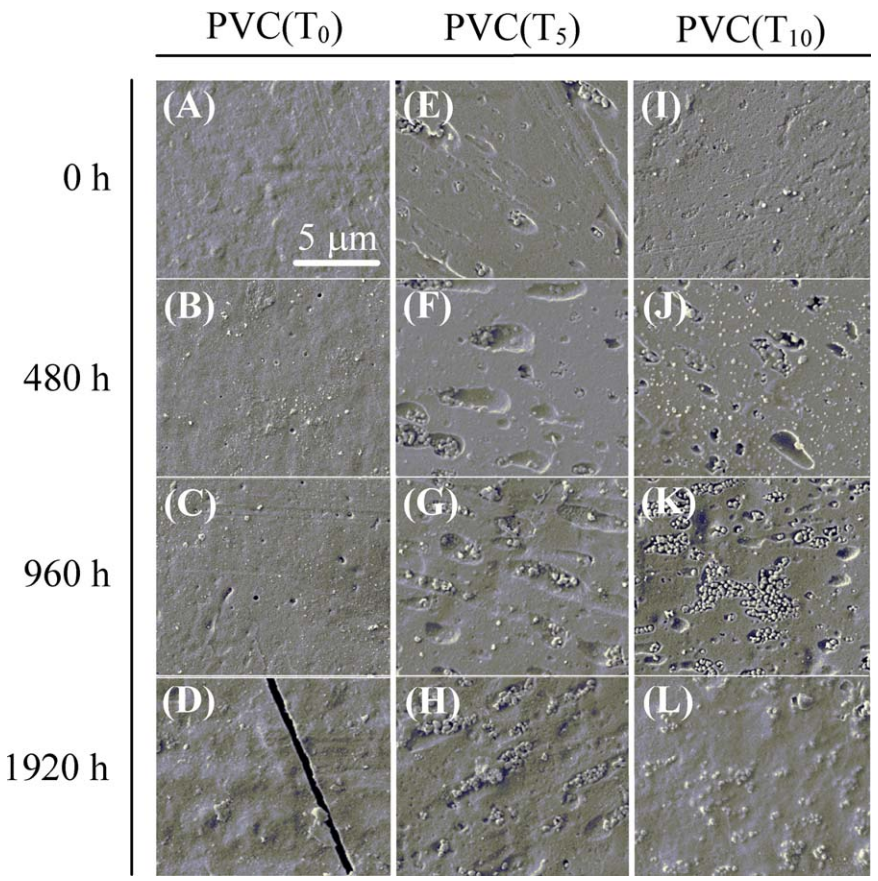

FIG. 1. SEM images of various composites over 1920 h of accelerated weathering. (A–D): PVC(T_0), (E–H): PVC(T_5), and (I–L): PVC(T_{10}). [Color figure can be viewed at wileyonlinelibrary.com]

generated a remarkable crack of width of approximately 1 μm caused by the sample preparation for SEM (Fig. 1D). This phenomenon is attributed to the fact that cracks form easily in the embrittled layer. Raab et al. [8] reported that preferential attack at irregularities, e.g., chromophores, may lead to stress concentration and the formation of micro-cracks. In contrast, no micro-cracks were found for TiO_2 particle-loaded PVCs over the entire exposure period. The changes of the surface morphology of PVC with TiO_2 particle during accelerated weathering are shown in Fig. 1E–L. At 480 h of accelerated weathering, a few shallow voids were observed on the surfaces of PVC(T_5) and PVC(T_{10}), especially at the surrounding regions of the TiO_2 particles (Fig. 1F, J). The generation of such voids is due to the photocatalytic ability of TiO_2 under the simultaneous conditions of UV, oxygen, and water that causes degradation of the polymer surrounding the TiO_2 particles [22–24]. Therefore, the oxidized chemical constituents and TiO_2 particles at the PVC surface were removed from the exposed surface by water. A similar result was reported by Gardette et al. [25]. Those voids are remarkably developed on the surface of TiO_2 particle-loaded PVCs after 960 h of accelerated weathering; many exposed TiO_2 particles are found to be agglomerated in the voids (Fig. 1G, K). However, after 1920 h of accelerated weathering, the surfaces of PVC(T_5) and PVC(T_{10}) become relatively smooth, and the TiO_2 particles appear to be covered by the polymer matrix again, particularly for the PVC(T_{10}) (Fig. 1H, L). This degradation process for the surface of PVC with TiO_2 particle is consistent with the degradation mechanism of the paint films containing TiO_2 pigment after weathering [23]. Accordingly, TiO_2 particle affects the weatherability of PVC composites in two distinct and opposing ways, i.e., on one hand, TiO_2 particle acts as a UV absorber to protect the PVC matrix, and on the other hand, TiO_2 particle acts as a UV-activated oxidation catalyst to degrade the PVC composite surface layer.

DMA Properties

DMA has been widely used to estimate thermal resistance, macromolecular variation, and changes in the stiffness of polymer materials. In this study, Fig. 2 presents the E' and tan δ as a function of temperature for PVCs with and without TiO_2. The E' values of all the unweathered PVCs decreased with increasing temperature because of the increasing chain mobility of the PVC matrix (Fig. 2A).

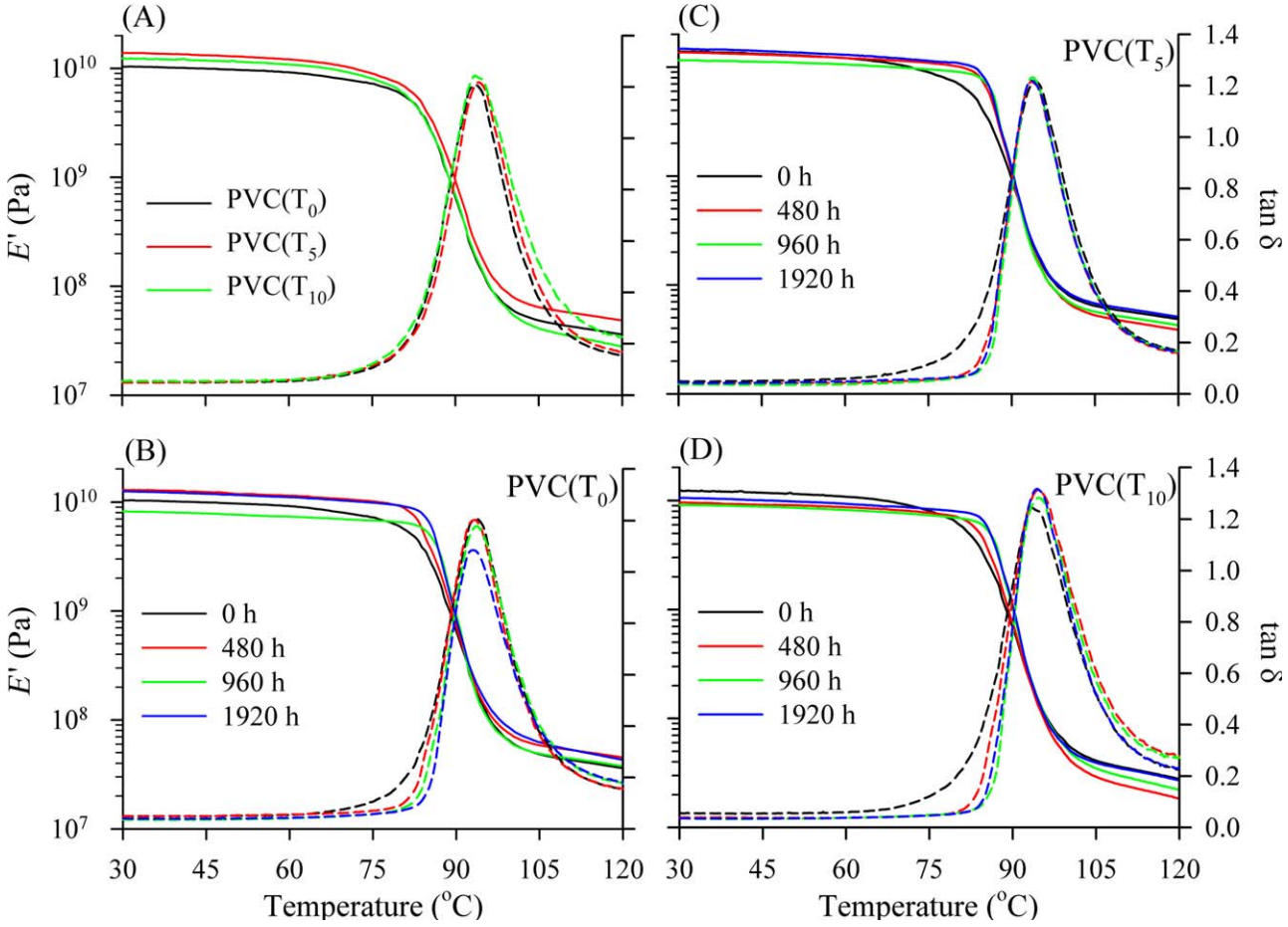

FIG. 2. Storage modulus (solid lines) and tan δ (dotted lines) of various composites before (A) and after (B–D) accelerated weathering. [Color figure can be viewed at wileyonlinelibrary.com]

A precipitous drop in E' can be expected near the glass transition temperature (T_g) of the PVC ($\sim$ 100 °C). Except for the width of the tan δ curve, there is no significant difference among the E' and the peak intensity of tan δ of the PVCs with different loading amounts of TiO_2 particle before weathering. A slight increase in the width of the tan δ curve was observed with increasing TiO_2 particle loading amounts in the PVC matrix, indicating the networks of PVCs with higher loading of TiO_2 particle exhibit a relatively heterogeneous structure. In addition, as shown in Fig. 2B, the intensity of tan δ decreased with increasing weathering time for PVC (T_0). The value of tan δ is an index of the macromolecular changes and the molecular motion of the material; as a result, the intensity of tan δ is correlated to the damping properties of the material. Accordingly, the PVC matrix is thought to undergo the crystallization or crosslink reaction, thereby causing embrittlement to the PVC (T_0) and leading to a decrease of the damping property. In contrast, the intensity of tan δ for PVCs with TiO_2 particle did not exhibit a remarkable decrease during the 1920 h of weathering; notably, for PVC(T_{10}), even a slight increase in the intensity of tan δ was observed after weathering (Fig. 2C, D). In other words, TiO_2 particle exhibits a good ability to inhibit the progression of damping loss for PVC composites during accelerated weathering. However, a narrow temperature range of tan δ was observed for all specimens beyond 480 h of accelerated weathering. This narrow glass transition can be attributed to the fact that the polymer networks exhibit relatively a homogeneous structure, while the broad glass transition occurs in the case of heterogeneous structure [26, 27]. Therefore, these results demonstrate that the polymer network of all PVCs undergoes a structural reorganization from a heterogeneous structure to a homogeneous network during the accelerated weathering.

Tensile Properties

The tensile test is widely used for determining the strength and ductility of a material, and the results are used as indices for new materials development and optimization [28]. In this study, no changes in the tensile yield stress (S_Y) and the yield elongation (E_Y) were observed for all specimens after accelerated weathering (data not shown). This phenomenon is consistent with the observations of Burn [13] that there is no great distinction

 DOI 10.1002/pc

TABLE 1. Ultimate tensile stress (S_U) and elongation at break (E_B) of various composites after accelerated weathering for 1,920 h.

	S_U (MPa)			E_B (%)		
Exposure time (h)	PVC(T_0)	PVC(T_5)	PVC(T_{10})	PVC(T_0)	PVC(T_5)	PVC(T_{10})
0	49.7 ± 1.6^{A}	47.4 ± 1.6^{A}	47.2 ± 1.3^{A}	118.8 ± 7.0^{A}	112.6 ± 6.1^{A}	119.8 ± 8.8^{A}
120	48.7 ± 1.3^{A}	49.4 ± 3.6^{A}	46.6 ± 4.6^{A}	110.5 ± 8.7^{AB}	114.7 ± 11.7^{A}	111.8 ± 13.6^{A}
240	46.9 ± 3.6^{AB}	49.6 ± 1.8^{A}	48.1 ± 2.1^{A}	102.6 ± 3.9^{B}	118.6 ± 6.8^{A}	116.1 ± 10.1^{A}
480	42.9 ± 3.1^{AB}	49.5 ± 2.4^{A}	48.1 ± 1.2^{A}	102.3 ± 3.1^{B}	123.2 ± 8.7^{A}	121.2 ± 4.2^{A}
960	39.5 ± 2.9^{B}	37.5 ± 2.5^{B}	44.2 ± 3.2^{A}	7.6 ± 4.9^{C}	39.2 ± 5.1^{B}	109.9 ± 4.6^{A}
1440	49.8 ± 4.5^{A}	39.3 ± 1.1^{B}	42.1 ± 6.9^{A}	2.5 ± 0.9^{C}	25.4 ± 5.9^{B}	100.7 ± 18.2^{A}
1920	48.8 ± 7.4^{A}	34.3 ± 2.2^{B}	43.1 ± 5.2^{A}	2.3 ± 0.7^{C}	25.1 ± 6.6^{B}	105.9 ± 8.0^{A}

Values are mean $\pm$ SD ($n = 5$). Different letters within a column indicate significant difference at $p < 0.05$.

for the yield tensile properties of PVC pipe with or without TiO_2 after natural weathering in Australia. In addition, Pabiot and Verdu [29] reported that the yield point of PVC film in the accelerated conditions with Xenon lamp, temperature, and rain simulation were practically invariant. The explanation for this observation is related to the fact that weathering of polymers generally causes degradation on the surface layer while leaving the bulk intact and thus has little effect on the bulk properties. Table 1 presents the ultimate tensile stress (S_U) of various specimens after accelerated weathering. For PVC(T_0), S_U decreased by approximately 20% (from 49.7 to 39.5 MPa) after 960 h of accelerated weathering. However, after 1,440 h of accelerated weathering, S_U suddenly increased to 49.8 MPa, which is almost equal to the initial break stress. S_U of PVC(T_5) also decreased by 20% to 37.5 MPa at 960 h of accelerated weathering and then leveled off; however, no significant differences were observed for PVC(T_{10}) over the entire exposure time. This result reveals that the loss of S_U decreased with increasing the loading amount of TiO_2 particle in the PVC matrix. In contrast, as presented in Table 1, the tensile elongation at break (E_B) for PVC(T_0) decreased remarkably with increasing exposure time. The tensile elongation at break decreased from 118.8% to 7.6% after 960 h of accelerated weathering, and then decreased to 2.5% after 1,440 h of accelerated weathering. This result was similar to the result of the study of Burn [13], which suggests that the weathering most likely formed a brittle, crosslinked, and degraded surface layer in which crazes can initiate. This explanation is supported by the DMA results in this study. As shown in Fig. 2B, the PVC(T_0) exhibits a remarkable loss of damping capacity at 1920 h of accelerated weathering, indicating the embrittlement of the PVC matrix. However, the E_B of PVC(T_5) exhibited a 65% decrease at 960 h of accelerated weathering and then leveled off (Table 1), which was a different trend of the results of PVC(T_{10}). The E_B of PVC(T_{10}) exhibited no significant changes during the entire exposure time. These results indicated that only sufficient amounts of TiO_2 particle (10 phr) in PVC composites could effectively prevent the loss of tensile properties during the accelerated weathering. However, one observation of interest is that the rheological behavior of PVC(T_0) was observed to significantly change from ductile to brittle during weathering. Figure 3 shows that the stress–strain behavior of PVC(T_0) is strongly dependent on the exposure time. PVC(T_0) is a ductile and tough material before weathering. However, the E_B of PVC(T_0) declined dramatically with increasing exposure time. As shown in Fig. 4, the S_Y and E_Y curves merged with the S_U and E_B curves, respectively, at the period of 960 h to 1440 h of accelerated weathering. This behavior reveals that the ductile behavior completely changes to the brittle behavior during this period for the weathered PVC(T_0).

Impact Properties

Pendulum impact testing (Charpy and Izod) is commonly used to measure the reduction in toughness of polymer materials caused by weathering. However, the sampling of the test specimens, especially the weathered thin samples, easily causes additional damage on the surface layer [30]. Therefore, the puncture impact test is an applicable method for polymer sidings and is used in the

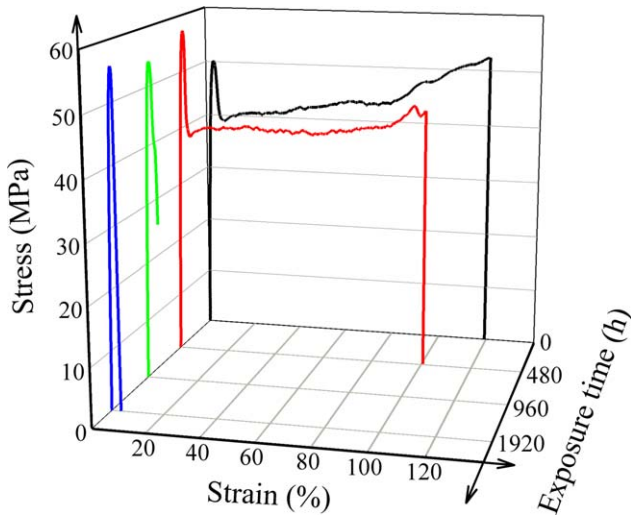

FIG. 3. Stress–strain curves of PVC(T_0) after accelerated weathering for 0 h, 480 h, 960 h, and 1920 h. [Color figure can be viewed at wileyonlinelibrary.com]

present study, because it is not necessary to obtain a specific notched or bar-shaped specimen before testing. Figure 5 shows changes in the MFE of all PVC composites as a function of exposure time. The initial MFE values of PVC(T_5) and PVC(T_{10}) were observed to be higher than that of PVC(T_0) by 21% and 13%, respectively. This result indicated that PVC with TiO_2 particle exhibits better impact properties, which is most likely due to TiO_2 particle acting as a reinforcement. However, no appreciable increase of MFE was observed for PVC with an increase in the TiO_2 particle amount. The MFE of PVC(T_0) exhibited no significant change up to 240 h (~20 J), and then dropped dramatically by 70% and 83% at 960 h and 1920 h, respectively. In contrast, the MFE of PVC(T_5) only decreased by 15% at 480 h, and then leveled off. When 10 phr of TiO_2 particle was added in PVC matrix, the MFE exhibited nearly no apparent change during the entire exposure time.

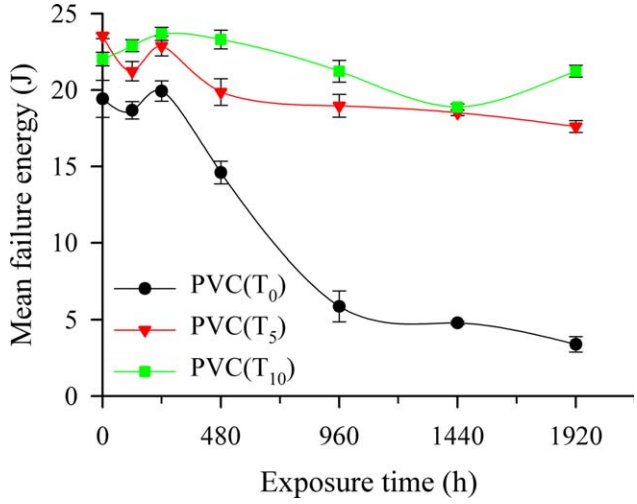

FIG. 5. The mean failure energy of all PVC composites over 1920 h of accelerated weathering. Values are mean ± SD ($n = 5$). [Color figure can be viewed at wileyonlinelibrary.com]

CONCLUSIONS

A few shallow voids in the regions surrounding the TiO_2 particles were developed on the weathered surfaces of PVC(T_5) and PVC(T_{10}), while only a roughened surface was observed for PVC(T_0). However, PVC composites without TiO_2 particles exhibited a ductile-brittle transition after 960 h of accelerated weathering. The E_B and MFE of PVC(T_0), originally 118.8% and 19.4 J, respectively, decreased dramatically after weathering for 1920 h to 2.3% and 3.4 J, respectively. With the addition of TiO_2 particle into the PVC composites, especially the case of PVC(T_{10}), not only E_B and MFE but also tan δ intensity and tensile property exhibited no significant differences before and after weathering. These results demonstrated that TiO_2 particle affects the weatherability of PVC composites in two distinct and opposing ways, i.e., TiO_2 particle acts simultaneously as a UV screener/absorber to protect PVC matrix and as a UV-activated oxidation catalyst to degrade the PVC surface layer. However, in spite of the photoreactive nature, at 10 phr loading level, TiO_2 particle could effectively protect the bulk polymer matrix from photodegradation during the QUV accelerated weathering. These results implied that high TiO_2 particle-loaded PVC composites should have a long service life time during outdoor weathering, which warrants further examination in future studies.

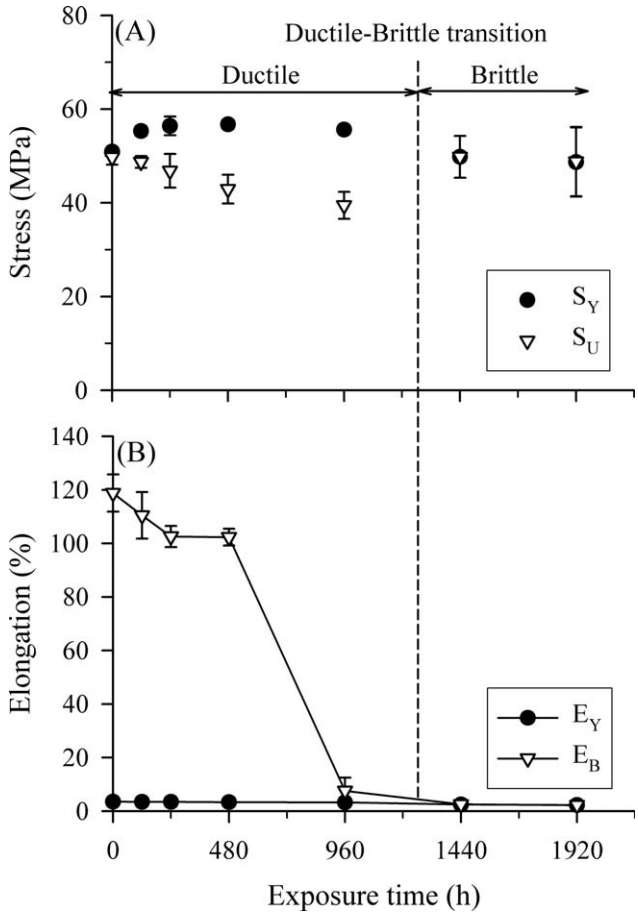

FIG. 4. Characteristic of ductile–brittle transition of PVC(T_0) after accelerated weathering. (A) Ultimate tensile stress (S_U) and yield (S_Y); (B) elongation at break (E_B) and yield (E_Y). Values are mean ± SD ($n = 5$).

REFERENCES

1. Chemical Division, Ministry of Economy, Trade and Industry, Japan, Forecast of Global Supply and Demand Trends for Petrochemical Products (2013). Available at: http://www.meti.go.jp/english/press/2013/0430_02.html. Last accessed October 13, 2014.
2. J. Leadbitter, J.A. Day, and J.L. Ryan, *PVC: Compounds, Processing and Applications*, iSmithers Rapra Publishing, United Kingdom (1994).
3. C. Decker, *Eur. Polym. J.*, **20**, 149 (1984).
4. J.L. Gardette and J. Lemaire, *Polym. Degrad. Stabil.*, **16**, 147 (1986).

 DOI 10.1002/pc

5. J.L. Gardette, S. Gaumet, and J. Lemaire, *Macromolecules*, **22**, 2576 (1989).
6. E.B. Rabinovitch, J.W. Summers, and W.E. Northcott, *J. Vinyl Technol.*, **15**, 214 (1993).
7. E.L. Bedia, M.A. Paglicawan, C.V. Bernas, S.T. Bernardo, M. Tosaka, and S. Kohjiya, *J. Appl. Polym. Sci.*, **87**, 931 (2003).
8. M. Raab, L. Kotulák, J. Kolaŕík, and J. Pospíšil, *J. Appl. Polym. Sci.*, **27**, 2457 (1982).
9. C. Anton-Prinet, G. Mur, M. Gay, L. Audouin, and J. Verdu, *Polym. Degrad. Stabil.*, **61**, 211 (1998).
10. J.L. Gardette and J. Lemaire, *Polym. Degrad. Stabil.*, **34**, 135 (1991).
11. J.W. Summers and E.B. Rabinovitch, *J. Vinyl Technol.*, **5**, 91 (1983).
12. J.L. Gardette and J. Lemaire, *Polym. Degrad. Stabil.*, **33**, 77 (1991).
13. L.S. Burn, *Polym. Degrad. Stabil.*, **36**, 155 (1992).
14. L.P. Real, A.P. Rocha, and J.L. Gardette, *Polym. Degrad. Stabil.*, **82**, 235 (2003).
15. R.E. Day, *Polym. Degrad. Stabil.*, **29**, 73 (1990).
16. N.S. Allen and H. Katami, *Polym. Degrad. Stabil.*, **52**, 311 (1992).
17. H.G. Völz, G. Kämpf, and H.G. Fitzky, *Prog. Org. Coat.*, **2**, 223 (1974).
18. M.H.S. Magdy, A.H. Yousry, and K.A.-M. Yasser, *Polym. Compos.*, **29**, 1049 (2008).
19. Z. Zhang, S. Wang, and J. Zhang, *Polym. Compos.*, **35**, 2365 (2014).
20. C. Anton-Prinet, G. Mur, M. Gay, L. Audouin, and J. Verdu, *Polym. Degrad. Stabil.*, **60**, 265 (1998).
21. T.-C. Yang, T. Noguchi, M. Isshiki, and J.-H. Wu, *Polym. Degrad. Stabil.*, **104**, 33 (2014).
22. M. Edge, C.M. Liauw, N.S. Allen, and R. Herrero, *Polym. Degrad. Stabil.*, **95**, 2022 (2010).
23. J.H. Braun, *Prog. Org. Coat.*, **15**, 249 (1987).
24. L.P. Real, J.L. Gardette, and A.P. Rocha, *Polym. Degrad. Stabil.*, **88**, 357 (2005).
25. J.L. Gardette and J. Lemaire, *J. Vinyl Technol.*, **15**, 113 (1993).
26. T. Xie and I.A. Rousseau, *Polymer*, **50**, 1852 (2009).
27. M.C.S. Perera, U.S. Ishiaku, and Z.A.M. Ishak, *Polym. Degrad. Stabil.*, **68**, 393 (2000).
28. S. Lampman, Characterization and Failure Analysis of Plastics, ASM International, Ohio, USA (2003).
29. J. Pabiot and J. Verdu, *Polm. Eng. Sci.*, **21**, 32 (1981).
30. J.R. White, "A Critical Assessment of Techniques for Monitoring Polymer Photodegradation," in *Service Life Prediction of Polymeric Materials–Global Perspectives*, J.W. Martin, R.A. Ryntz, J. Chin, and R.A. Dickie, Eds., Springer, New York, USA (2006).